Mathematical Description and Control Design for the Simultaneous Levitation and Propulsion of a Conveyor Vehicle

Thomas Herold
Institute of Electrical Machines
RWTH Aachen University
52056 Aachen, Germany
Email: thomas.herold@iem.rwth-aachen.de

André Pohlmann
Institute of Electrical Machines
RWTH Aachen University
52056 Aachen, Germany

Kay Hameyer
Institute of Electrical Machines
RWTH Aachen University
52056 Aachen, Germany

***Abstract*—Magnetic levitation is still an important issue for industry and research. Wherever high dynamics, position accuracy, high reliability and low mechanical wear are required, magnetic levitation is an effective alternative to conventional technologies. Conventional systems with mechanical guiding have shown to be limited in speed. For transporting goods over long distances, levitation can thus lead to a significant saving in time and cost. This paper describes a control design for an autonomous magnetically levitated conveyor vehicle with a linear direct drive for propulsion. Based on a mathematical description as a 2-rigid-body system with elastic coupling in torsion, a simulation environment for the vehicle is created. After that, a degree-of-freedom control is designed for the levitation operation, whereas a conventional PI control is used for the propulsion. This control design is based on the representation of the system as a 2-body system as well. The combination of control and simulation environment offers the opportunity for extensive testing and optimization before the control is applied to a test bench. By intensive analysis the stable and efficient operation of the vehicle is determined. An assortment of measurement results is presented and discussed in this paper.**

I. Introduction

Globalization goes along with increasing transportation and traffic, which requires more and more efficient conveyance technology. Especially in air transportation there is a need for improving existing capacities. In particular, an increase in the number of passengers calls for an acceleration in luggage handling. Conventional conveyor vehicles (e.g. AUTOVER, BAGTRAX) are however limited in their maximum speed because of the mechanical guiding. A further development of transportation capacities is possible by using magnetic levitation technology. In previous publications [1], [2], an autonomous magnetically levitated conveyor vehicle is described. Due to its also contact-free operating linear drives, a speed beyond 10 m/s becomes possible. In this paper, a new control design is presented, which enhances the dynamics and the stability of this system. In a first step, a mathematical description of the vehicle as a 2-rigid-body system is established. Derived from this description, a simulation model is build in Matlab/Simulink, which accounts for the non balanced propulsion and cogging forces of the drive. Thereupon, the control design is performed and tested within the simulation environment. After successful tests the control is applied to a test bench and its validity proven by various experiments. As a result, a stable levitation with simultaneous propulsion is reached. Additionally to the control aspects this paper provides a impression of the power consumption of the overall system.

II. The Conveyor Vehicle

The vehicle (Fig. 1) consists of a H-shaped aluminum frame with a levitation/propulsion head at each corner. For mechanical stabilization an aluminum plate, which additionally serves as loading platform, is mounted on the top of the carrier.
The levitation magnets consist of a classical U-shaped magnetic core with permanent magnets on top of each arm and two coils for producing an adjustable attraction force. The linear drives for propulsion are located exactly below the levitation magnets (See Fig. 2). They have a synchronous homopolar design with a permanent magnet excitation (Fig. 3). To provide a high excitation flux the motor has two opponent installed actuators, one above and one under the flux guiding, attached to one iron yoke. This design provides a high power density, despite the large air gap. Since the active part of the motors are mounted on the vehicle, the track is completely passive and consists only of the levitation rails and the flux guides. With a system of three light barriers per motor it is possible to identify the rotor angle by detecting the gaps between the flux guides with a resolution of 60 degrees (elec.) - sufficient for a six-step commutation. Furthermore, this angle detection is used as an incremental positioning system.
Unfortunately, this kind of motor produces high cogging forces, that have to be considered during the control design process (section IV), and has appreciable eddy current losses. To reduce this losses it is imaginable to install the secondary motor parts only in the areas where acceleration and deceleration is required.

III. Mathematical Description and Modeling

The mathematical description of the conveyor vehicle consists of mechanical and electromagnetic aspects. For describ-

978-1-4244-4252-2/09/$25.00 ©2009 IEEE

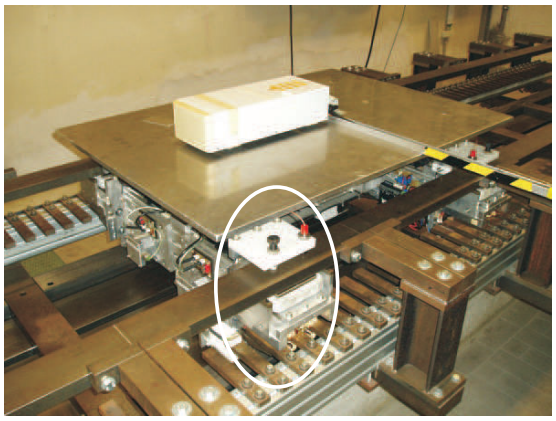

Fig. 1. The conveyor vehicle in its track.

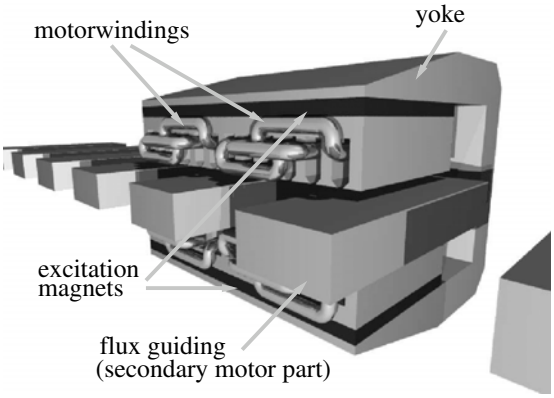

Fig. 3. The homopolar motor.

ing the vehicle mechanics a Cartesian coordinate system is of advantage since it is able to describe the global values of the vehicle like mass or the moment of inertia. Because some values are dependent on local quantities (e.g. the airgaps between the levitation magnet and the rail) a transformation between the local and the global coordinates has to be determined. This chapter shows the mathematical abstraction of the system consisting of the mechanics, the hybrid magnets and linear drives and the coupling of the two coordinate systems.

A. Mechanical Model

For the purpose of dynamical modeling the vehicle is described as a multi-body system (MBS) with two elastically coupled rigid bodies. This description uses Cartesian coordinates with the six degrees of freedom $x, y, z, \alpha, \beta, \gamma$ as suggested in [3]. These DOFs describe the translational movements in three directions and the rotations around the respective axes. Additionally, a further DOF is introduced to represent the torsion of the framework. The seven DOFs, of which the meaning is presented in Fig. 4, are combined in a vector

$$\mathbf{q} = (x \;\; y \;\; z \;\; \alpha \;\; \beta \;\; \gamma \;\; \delta)^T \tag{1}$$

to describe the global position of the vehicle. The governing equation of an MBS is [4]

$$\mathbf{M}\ddot{\mathbf{q}} + \mathbf{P}\dot{\mathbf{q}} + \mathbf{Q}\mathbf{q} = \mathbf{f} \quad , \tag{2}$$

where $\mathbf{M}$, $\mathbf{P}$ and $\mathbf{Q}$ are the mass, damping and stiffness matrices and $\mathbf{f}$ the excitation forces. In this equation the magnetic levitation forces, the damping forces due to the eddy-currents induced in the track and the position dependent propulsion and cogging forces (Fig. 6), which have been calculated by the finite element method in a previous research [5], [6], are considered.

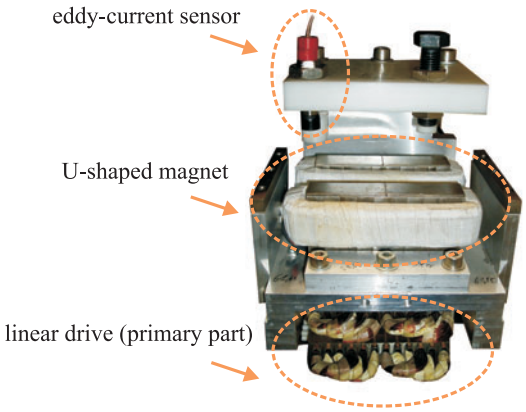

Fig. 2. One levitation/propulsion head of the vehicle.

B. Modeling of the Hybrid Magnets and the Linear Motors

For the modeling of the hybrid magnet the equation of the magnetic forces as well as the differential equation of the magnetomotive force in the coils are required. The first equation is obtained by the Taylor expansion with break-off behind the second term to express a linear correlation between the force F_{mag}, the airgap d and the magnetomotive force θ around a specific working point:

$$F_{mag}(\theta, d) = F_{mag}(\theta_0, d_0) + (\theta - \theta_0) \cdot \left.\frac{\partial F_{mag}}{\partial \theta}\right|_{\theta_0, d_0} + (d - d_0) \cdot \left.\frac{\partial F_{mag}}{\partial d}\right|_{\theta_0, d_0} \quad . \tag{3}$$

In the operating point the derivatives in (3) are constant values. For this reason they are replaced by the coefficients $k_{d,mag}$ and $k_{\theta,mag}$. Furthermore, Δ-values are introduced to describe deviations from the operating point:

$$\left.\frac{\partial F_{mag}}{\partial d}\right|_{\theta_0, d_0} = k_{d,mag}, \qquad \left.\frac{\partial F_{mag}}{\partial \theta}\right|_{\theta_0, d_0} = k_{\theta,mag}$$
$$(d - d_0) = \Delta d, \qquad (\theta - \theta_0) = \Delta\theta \quad . \tag{4}$$

By using these abbreviations and renaming the static term $F_{mag}(\theta_0, d_0)$ to $F_{mag,0}$, (3) can be expressed as

$$F_{mag}(\theta, d) = F_{mag,0} + k_{\theta,mag} \cdot \Delta\theta + k_{d,mag} \cdot \Delta d \quad . \tag{5}$$

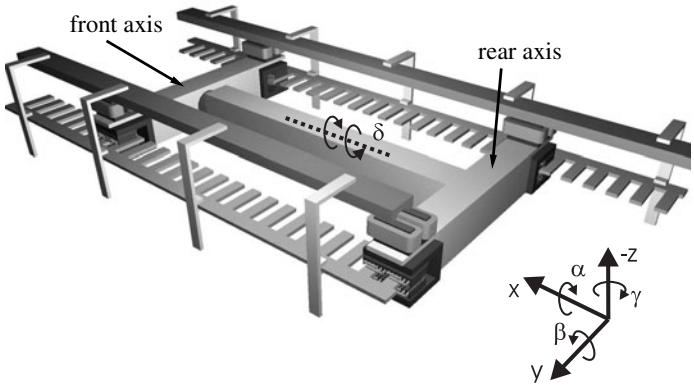

Fig. 4. Relation of the global coordinates to the vehicle.

The equation for the magnetomotive force is obtained using the Kirchhoff's voltage law containing an ohmic voltage drop and a magnetic induced voltage:

$$u = R \cdot \frac{\theta}{N} + N \cdot \frac{d\phi(\theta, d)}{dt} \quad . \tag{6}$$

The symbol N represents the number of turns of the coils. Here the Taylor expansion is used again to linearize the flux near the operating point:

$$\begin{aligned} \phi(\theta, d) = \phi(\theta_0, d_0) + (\theta - \theta_0) \cdot \left.\frac{\partial \phi}{\partial \theta}\right|_{\theta_0, d_0} \\ + (d - d_0) \cdot \left.\frac{\partial \phi}{\partial d}\right|_{\theta_0, d_0} \end{aligned} \quad . \tag{7}$$

As well as (5) the flux formula is reduced by using Δ-values and the constant coefficients $k_{\theta,phi}$ and $k_{d,phi}$ and renaming the static term $\phi(\theta_0, d_0)$:

$$\phi(\theta, d) = \phi_0 + k_{\theta,phi} \cdot \Delta\theta + k_{d,phi} \cdot \Delta d \quad . \tag{8}$$

In a further step this flux is inserted into (6). After solving and rearranging, the differential equation of the magnetomotive force is determined:

$$\Delta\dot{\theta} = \frac{1}{N k_{\theta,phi}} \cdot u - \frac{R}{N^2 k_{\theta,phi}} \cdot \theta - \frac{k_{d,phi}}{k_{\theta,phi}} \cdot \Delta\dot{d} \quad . \tag{9}$$

To obtain a variable levitation force, the control has to vary the voltage in this equation. For delivering the necessary power a converter is switched between the control signal and the coils. Since this converter possesses an integrated current controller, equation (9) has to be adjusted. At first the speed dependent term can be neglected because the time constant of the current control is smaller than the mechanical one by far. Furthermore, a gain value, K, is introduced that describes the ratio between output current and the voltage input signal. Due to a high DC link voltage, the time constant of the magnetomotive force is reduced to T. Altogether, the equation of the magnetomotive force becomes

$$\Delta\dot{\theta} = \frac{NK}{T} \cdot u - \frac{1}{T} \cdot \theta \quad . \tag{10}$$

The model of the linear drives also contains an electrical and a mechanical component. Since the electrical one has a similar description as the according component of the hybrid magnet it is not enlarged.

As aforementioned, the position dependent propulsion and cogging forces have to be considered. This is done by introducing a shape function $k_{\theta,prop}(x)$ and a term for the cogging forces, which have been derived from the simulation results shown in Fig. 6:

$$F_{prop}(x) = k_{\theta,prop}(x) \cdot \theta_{prop} + F_{cog}(x) \quad . \tag{11}$$

C. Coupling of local and global Quantities

The position of the conveyor vehicle is described in Cartesian coordinates whereas the magnetomotive and mechanical forces of the magnets and motors are local quantities. For the description of the overall vehicle system a transformation between this local and global quantities is required. For this purpose the two transformation matrices $\mathbf{J}_{AB}$ and $\mathbf{J}_{BA}$ are introduced and their derivation exemplified with the torsion angle δ. The used indices A and B represent local and global values respectively.

As shown in Fig. 5 the torsional forces distort the front and rear axis of the vehicle against each other. The torsion angle can be expressed by

$$\sin(\delta) = \frac{1}{a}(-\Delta d1 + \Delta d2 - \Delta d3 + \Delta d4) \quad , \tag{12}$$

where Δd_i are the deviations of the air gaps from their operating point and a the distance between the magnets at the front and rear axis. With the small-angle approximation $\sin(x) \approx x$, (12) is reduced to

$$\delta = \frac{1}{a}(-\Delta d1 + \Delta d2 - \Delta d3 + \Delta d4) \quad . \tag{13}$$

The other DOFs are determined in the same way, which leads to the Jacobean matrix

$$\mathbf{J}_{AB} = \frac{\partial \mathbf{q}}{\partial \Delta \mathbf{d}_A^T} = \frac{\partial (x \;\; y \;\; z \;\; \alpha \;\; \beta \;\; \gamma \;\; \delta)^T}{\partial (d_1 \;\; d_2 \;\; d_3 \;\; d_4 \;\; d_{x1} \;\; d_{x2} \;\; d_y)} \quad . \tag{14}$$

The values $d_1 ... d_4$ represent the airgaps of the levitation system, whereas d_{x1}, d_{x2} and d_y describe the displacement of the motors in x and y direction. The back-transformation $\mathbf{J_{BA}}$ is obtained by inversion of the matrix (14). Since there is only a negligible coupling between the levitation and the propulsion system, it is possible to separate the levitation dependent part

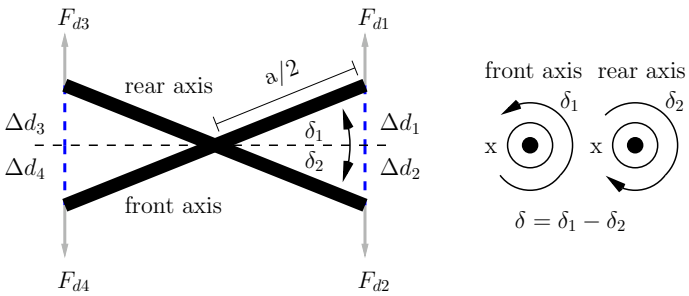

Fig. 5. Torsion of the conveyor vehicle.

from the transformation matrices as well as the propulsion dependent part. This transformations are valid for all quantities except the forces, for which the transformation is obtained by similar considerations. The resulting matrix is formal equal to $\mathbf{J}_{BA}^T$:

$$\mathbf{J}_{ABforce} = \mathbf{J}_{BA}^T = (\mathbf{J}_{AB}^{-1})^T \tag{15}$$

IV. Control Design

The control system of the vehicle is separated into two parts: the levitation system with a DOF control scheme on the one hand, and a conventional PI control for the propulsion on the other hand.

A. Levitation Control

Uncontrolled magnetic levitation represents an unstable system. This is based on the negative stiffness of the levitation magnets, wherefore the zero/pole diagram of one actuator shows a pole with a positive real value. To achieve a stable operation, a controller has to be employed that eliminates the pole on the positive half plane. Two designs are feasible: one separate controller for each airgap or one controller for each DOF like suggested in [7]. The single magnet control has the disadvantage of disturbance transmissions between the four levitation magnets of the vehicle due to the mechanical coupling by the frame. With the DOF controller this coupling is loosened into the independent degrees of freedom in (1). Hence, this control scheme is chosen. However, with four actuators only four of this seven DOFs are controllable. These DOFs are the vertical position, the rotations around the cross and the direct axis and the torsion, combined in the vector

$$\tilde{\mathbf{q}} = (z \;\; \alpha \;\; \beta \;\; \delta)^T \quad . \tag{16}$$

From the missing DOFs, the lateral guiding is completely passive, thanks to reluctance forces, i.e. y is not controlled. The propulsion and the yawing (x, γ) are controlled by the linear drives.

In the next step the controllers of each DOF in $\tilde{\mathbf{q}}$ are designed. For the topology the PI-state control [8] has been found as appropriate. The synthesis of the controllers is shown in the following by dwell on δ exemplary.

Since the DOFs are not directly measurable, they are calculated from four signals representing the gaps between the actuator and the rails. These airgaps (d_i) are measured with eddy-current sensors (Fig. 2) and represent local quantities that have to be transformed into global coordinates

$$\tilde{\mathbf{q}} = (z \;\; \alpha \;\; \beta \;\; \delta)^T = \tilde{\mathbf{J}}_{AB} \cdot (d_1 \;\; d_2 \;\; d_3 \;\; d_4)^T \tag{17}$$

with the transformation matrix $\tilde{\mathbf{J}}_{AB}$, which is the levitation dependent part of (14). The same counts for the other local quantities like speed and magnetomotive and mechanical forces. The starting point of the control design is the global force equation, that is derived from the local forces by neglecting the gravity and the static magnetic forces:

$$\begin{aligned}\mathbf{f}_B &= (F_z \;\; T_\alpha \;\; T_\beta \;\; T_\delta)^T = \tilde{\mathbf{J}}_{ABforce} \cdot \mathbf{f}_\mathbf{A} = \tilde{\mathbf{J}}_{BA}^T \cdot \mathbf{f}_\mathbf{A} \\ &= k_{\theta,mag} \cdot \tilde{\mathbf{J}}_{BA}^T \cdot \boldsymbol{\Delta\theta_A} + k_{d,mag} \cdot \tilde{\mathbf{J}}_{BA}^T \cdot \mathbf{\Delta d_A}\end{aligned} \quad . \tag{18}$$

By means of further transformations and the MBS equation (2) this formula is solved to

$$\begin{aligned}\ddot{\mathbf{q}} = \mathbf{M}_{B,(C)}^{-1} \cdot (&k_{\theta_{mag}} \cdot \tilde{\mathbf{J}}_{BA}^T \cdot \tilde{\mathbf{J}}_{BA} \cdot \Delta\boldsymbol{\theta}_B \\ &+ k_{\delta_{mag}} \cdot \tilde{\mathbf{J}}_{BA}^T \cdot \tilde{\mathbf{J}}_{BA} \cdot \mathbf{q})\end{aligned} \quad . \tag{19}$$

If expressed element-wise, (19) represents an independent equation for each DOF. Hence, $\ddot{\delta}$ becomes

$$\ddot{\delta} = \frac{1}{I_T}(\underbrace{a^2 \cdot k_{\theta_{mag}}}_{k_\theta^\delta} \cdot \Delta\theta_\delta + \underbrace{a^2 \cdot k_{d_{mag}}}_{k_d^\delta} \cdot \delta) \quad . \tag{20}$$

In the next step the state vector is defined to

$$\mathbf{x}_\delta = (\delta \;\; \dot{\delta} \;\; \Delta\theta_\delta)^T \tag{21}$$

with the torsion δ, its deviation $\dot{\delta}$ and the magnetomotive force $\Delta\theta_\delta$ of the coils transformed to global quantities. Now, with (20), (21), (10) and (14) it is possible to form the state equations to

$$\begin{pmatrix} \dot{\delta} \\ \ddot{\delta} \\ \Delta\dot{\theta}_\delta \end{pmatrix} = \underbrace{\begin{pmatrix} 0 & 1 & 0 \\ \frac{k_d^\delta}{I_T} & 0 & \frac{k_\theta^\delta}{I_T} \\ 0 & 0 & -\frac{1}{T} \end{pmatrix}}_{\mathbf{A}_\delta} \begin{pmatrix} \delta \\ \dot{\delta} \\ \Delta\theta_\delta \end{pmatrix} + \underbrace{\begin{pmatrix} 0 \\ 0 \\ \frac{NK}{T} \end{pmatrix}}_{\mathbf{B}_\delta} \cdot u_\delta$$

$$\delta = \underbrace{\begin{pmatrix} 1 & 0 & 0 \end{pmatrix}}_{\mathbf{C}_\delta} \begin{pmatrix} \delta \\ \dot{\delta} \\ \Delta\theta_\delta \end{pmatrix} \quad . \tag{22}$$

Since the system has no feedthrough, the matrix $\mathbf{D}_\delta$ is equal to zero. With these state matrices the feedback gains are identified. This can be done by several approaches. In this paper the design is made by the method of Riccati followed by a fine adjustment using pole placement.

The output values of the controllers have to be transformed back to local actuator currents by

$$\begin{aligned}(I_1 \;\; I_2 \;\; I_3 \;\; I_4)^T &= K \cdot (u_1 \;\; u_2 \;\; u_3 \;\; u_4)^T \\ &= K \cdot \tilde{\mathbf{J}}_{AB}^{-1} \cdot (u_z \;\; u_\alpha \;\; u_\beta \;\; u_\delta)^T\end{aligned} \tag{23}$$

and are given to the power converters afterwards.

Contrary to the fast behavior of the controls for z, α and β the torsion control is set very slow. With such an adjustment δ has only a minor dynamical stiffness. This is done because this DOF is established to compensate static or low-frequency disturbances only. These are especially unbalanced load and moving along mechanical tolerances of the track. These alignments are for the purpose to minimize the required control energy.

B. Propulsion Control

Contrary to the high-precision eddy-current sensors of the levitation system, the propulsion control uses an optical incremental measurement, which detects the gaps between the secondary motor parts (Fig. 3). This system has a resolution of only 1cm for which reason a rotation around the vertical

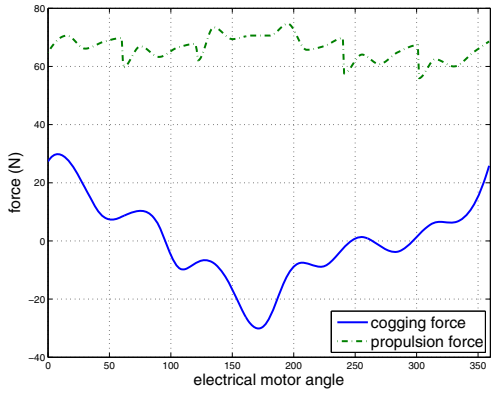

Fig. 6. The cogging and propulsion forces of the homopolar motor [5], [6].

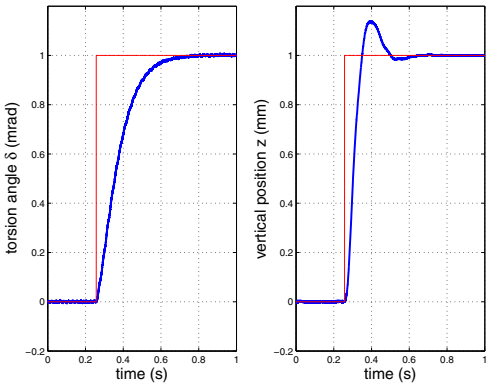

Fig. 7. Set point change of the DOFs δ and z.

axis (γ) is poorly measurable. Therefore, and because these rotations do not occur in a troublesome magnitude, this DOF is not controlled. The only remaining DOF is the feed x, that represents the position of the vehicle along the track. Here a conventional PI-cascade is chosen because there is no need for a high feed accuracy in a luggage transportation system. Furthermore, the resolution of the positioning system is to low for a proper compensation of the motor cogging forces (Fig. 6). Despite arranging the rear motors 180 electrical degrees shifted, which reduces the overall cogging forces in amplitude, there is only every 6 cm a stable position, if the motors are currentless. Due to efficiency, the nominal position is quantized to steps of also 6 cm to exclude stopping positions where motor currents would be needed to hold.

V. System Simulation

The levitation magnets and the propulsion are able to generate very high forces. With an insufficient control these forces may damage the mechanical parts of the vehicle. Therefore, the mathematical description from section III as well as the control is cloned in a graphic programmable ODE solver (Simulink). This provides the opportunity to perform an overall simulation, which is used to test the control for its capability and to adjust the control parameters for a stable and precise operation. Moreover, these simulations provide an insight into the system behavior before applying the control to the test bench.

VI. Results

This section describes the measurement results of the test bench. This includes the control behavior and the power consumption of the system.

A. Control Behavior

In order to assess the capabilities of the developed control, multiple experiments are performed. This includes, for example, raising the vehicle while launching the levitation system. Furthermore, many load scenarios are analyzed to simulate the process of charging the platform with its load, e.g. a suitcase. All of these experiments have given satisfactory results with respect to stability.

In Fig. 7 a set point change in the DOFs δ and z is shown. They rise from zero to 1 mrad in δ and 1 mm in z respectively. As mentioned in section IV the torsion control is designed to be very slow. While the jump in z raises all airgaps for 1 mm, what takes a tenth of a second, the torsion of 1 mrad means only a change of 0.4 mm in each airgap. Nevertheless, it takes approx. half a second to reach the new set point. Thus, the torsion control operates as desired. Furthermore, the diagram shows an overshot in z. It has its reason in the unbalanced mass distribution of the vehicle, which causes different accelerations of the four vehicle corners. Even if a slower control design can reduce the overshot the dynamic is more important. Besides, an overshot of 15% does not affect the system operation.
The characteristics of the propulsion system and its influence on the levitation are investigated by accelerating and moving the vehicle along the track. The measurements of a set point change of 2 m are displayed in Fig. 8. While the DOF x shows the desired behavior (Fig. 8(a)), in z many deviations from the set point (i.e. z=0) can be seen (Fig. 8(b)). They do not have their origin in force impacts of the linear drives but are caused by disturbances of the eddy-current sensors. This is due to the fact that the rails are not made in one piece but assembled from many short parts. The appearing joints induce discontinuities in the eddy-current response. Passing by such a joint leads to measurement errors that cause the disturbance in z. In the DOFs α, β and δ this behavior occurs as well. Nevertheless, the operation of the entire system is not affected because the nominal air gap is designed to 3 mm. Thus, a sufficient buffer is provided.

B. Power Consumption

An important aspect of a conveying system is its power consumption. Especially an increase of the transportation speed leads to a higher energy absorption. The whole power consumption consists of four parts: copper losses, iron losses, losses of the electronic periphery and air friction losses. Up to 10 m/s the air friction can be neglected. The periphery has all about the same power consumption in every operational point of ca. 130 W. In the following the copper and iron losses are examined separately for the levitation and the propulsion.

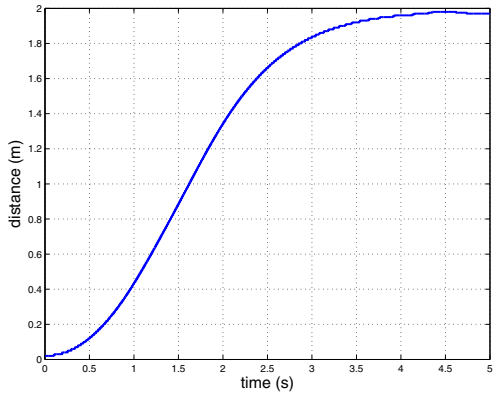

(a) Reaction on set point change of DOF x.

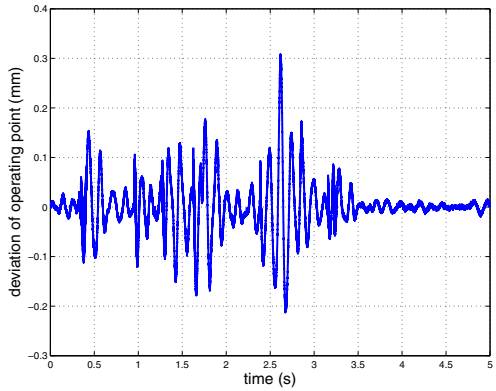

(b) Influence of motion in x to z.

Fig. 8. Set point change of the feed and its influence on the levitation system.

1) Levitation Losses: At zero speed the levitation system has only copper losses from the four levitation magnets. Because the levitation force is adjustable by changing the air gap it is possible, even at maximum load, to keep the coil current near zero that the losses almost vanish. With movements of the vehicle the control has to compensate disturbances, which requires more energy. Fig. 9 show the influence of such disturbances on the power consumption at a set point change of the propulsion of 2 m. At standstill and very low speeds the absorbed power consists only of the static electronic input power of approximately 30 W. With higher speeds the disturbance grows, especially because of the mechanical joints of the rails, and the power reaches over 100 W maximum. The average input power of the levitation system is 43 W, which means that the average compensation power is only 13 W. This value will increase with the speed. But the more relevant losses are the iron losses. In [5] it is shown that the eddy current losses amount to 200 W at 10 m/s for all four magnets.

2) Propulsion Losses: The iron losses of the linear drives will increase from zero at standstill to 300 W at 10 m/s [5]. To compensate the overall iron losses of the system at this speed the propulsion has to produce a force of

$$F = \frac{P_{iron}}{v} = \frac{500\,\mathrm{W}}{10\,\mathrm{m/s}} = 50\,\mathrm{N} \quad . \tag{24}$$

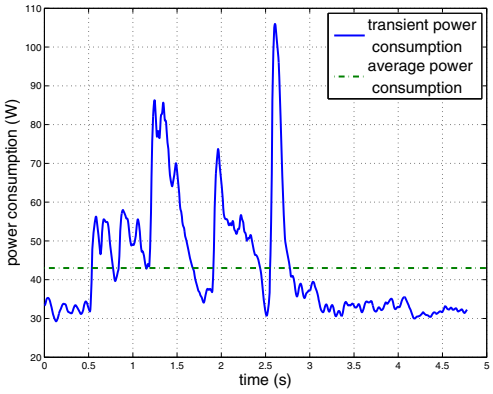

Fig. 9. Power consumption of the levitation system.

This means that the copper losses are only 20 W at constant speed.
The overall power consumption of the system at 10 m/s is calculated to approx. 800 W.

VII. Conclusion

This paper describes the mathematical modeling of a magnetically levitated conveyor vehicle system and the design of its control. Using established methods the control is derived from the mathematical equations. The proper operation of the system in combination with the control is proven - a stable levitation operation by simultaneous use of the propulsion is obtained. All measurements show, that the requirements for a conveying system are fulfilled. Furthermore, an insight in the power consumption of the system is given.

References

[1] J. Van Goethem. *"Verlustarme magnetische Lagerung für ein Förderfahrzeug mit normalkraftbehaftetem Linearantrieb"*, Ph.D. dissertation, Institute of Electrical Machines, RWTH Aachen University, Shaker Verlag, 2004.

[2] D. Brakensiek. *"Lineares Antriebssystem für ein magnetisch gelagertes Transportsystem"*, Ph.D. dissertation, Institute of Electrical Machines, RWTH Aachen University, Shaker Verlag, 2004.

[3] J. Van Goethem, L. Schober, G. Henneberger. *"Design and Simulation of a Magnetic Levitation Conveyor Vehicle"*, Proceedings of the 7th International Conference on Modeling and Simulation of Electric Machines, Converters and Systems, August 2002.

[4] D.J. Ewins. *"Modal Testing: Theory, Practice and Applications"*, Research Studies Press LTD., 2000.

[5] M. Leßmann, K. Hameyer *"Computation Of Eddy Current Losses In The Mounting Rail Of A Magnetically Levitated Conveyor Vehicle"*, Proceedings of the 12th International Symposium on Electromagnetic Fields in Mechatronics, Electrical and Electronic Engineering, September 2005.

[6] D. Brakensiek, G. Henneberger, *"Design of a Linear Homopolar Motor for a magnetic levitating transportation vehicle"*, The 3rd International Symposium on Linear Drives for Industry Applications, October 2001.

[7] A. Schmidt, C. Brecher, F. Possel-Dölken. *"Novel Linear Magnetic Bearings for Feed Axes with Direct Drives"*, International Conference on Smart Machining Systems, March 2007.

[8] H. Beck, D. Turschner, *"Commissioning of a State-Controlled High-Powered Electrical Drive Using Evolutionary Algorithms"*, IEEE Transactions on Mechatronics, Vol.6, No.2, June 2001